European Radiology (2019) 29:1258–1266
https://doi.org/10.1007/s00330-018-5717-3

MUSCULOSKELETAL

Comparison of radiographs, tomosynthesis and CT with metal artifact reduction for the detection of hip prosthetic loosening

Romain Gillet[1] · Pedro Teixeira[1] · Chloé Bonarelli[1] · Henry Coudane[2] · François Sirveaux[3] · Mathias Louis[1] · Alain Blum[1]

Received: 17 May 2018 / Revised: 18 July 2018 / Accepted: 14 August 2018 / Published online: 7 September 2018

Abstract

Objectives To evaluate the diagnostic performance of digital tomosynthesis (DTS) for the diagnosis of hip prosthesis loosening (PL) compared with conventional radiographs and CT with metal artifact reduction (CT-MAR).

Methods Forty-nine patients with painful hip prosthesis were prospectively included and underwent anteroposterior and lateral radiographs, anteroposterior DTS and CT-MAR of the hip. This study was approved by the local ethics committee, and all patients signed an informed consent form. Images were evaluated independently by two radiologists. Periprosthetic radiolucent lines wider than 2 mm found in two or more Gruen or De Lee and Charnley zones were considered diagnostic of PL. All cases of PL were confirmed surgically. Patients with a stable radiological follow-up for at least 1 year with an alternative cause for the symptoms or with no surgical evidence of PL were considered PL negative.

Results There were 21 cases of PL, 9 unilateral and 12 bilateral. For both the acetabular and femoral sides, DTS had a specificity for PL detection similar to that of conventional radiographs and CT-MAR (98.5–100%, 96.9%–100% and 96.9–95.4% respectively for both readers) and a sensitivity similar to conventional radiographs (39.9–45.4% versus 33.3–51.5% for both readers) but lower than CT-MAR (84.85% for both readers). The interobserver agreement was 0.84 for CT-MAR, 0.53 for DTS and 0.39 for conventional radiographs.

Conclusion DTS has a similar diagnostic performance to radiographs for the diagnosis of PL with a better interobserver agreement. The sensitivity however remains lower than that of CT-MAR.

Key Points

- *Plain radiograph is still the first imaging step when hip prosthesis loosening is suspected.*
- *Interobserver agreement is better with digital tomosynthesis than radiographs.*
- *Sensitivity of CT with state-of-the-art metal artifact reduction is superior to that of digital tomosynthesis.*

Keywords Prosthesis loosening · Diagnostic techniques and procedures · Hip replacement arthroplasty · Interobserver variation · Tomography, x-ray computed

✉ Romain Gillet
romain_gillet3@hotmail.com

[1] Service d'Imagerie GUILLOZ, Hôpital Central, CHRU de Nancy, 29 Avenue du Maréchal de Lattre de Tassigny, 54000 Nancy, France

[2] Service d'Arthroscopie, Traumatologie et Orthopédie de l'Appareil Locomoteur, Hôpital Central, CHRU de Nancy, 54000 Nancy, France

[3] Centre Chirurgical Emile Gallé, CHRU de Nancy, 54000 Nancy, France

Abbreviations

BMI	Body-mass index
CT-MAR	Computed tomography with metal artifact reduction algorithms
DTS	Digital tomosynthesis
PL	Prosthesis loosening
RLZs	Radiolucent zones
Se	Sensitivity
Sp	Specificity
THA	Total hip arthroplasty

Introduction

Total hip arthroplasty (THA) is a frequently used procedure with high success rates. The number of THAs is expected to increase in the next decade [1]. Despite its good clinical outcomes, follow-up surgery is necessary in about 1% of all THA cases [2] due to mechanical loosening and wear in 42% and 11% of cases respectively in France [3]. Prosthesis loosening (PL) can be radiologically or clinically silent, hence the necessity for a reliable imaging method for early diagnosis in routine follow-up, especially in patients with hip pain [4, 5].

Conventional radiographs are the first imaging modality used for routine follow-up in cases of painful THA [6], but suffer from low sensitivity in depicting periprosthetic osteolysis due to superimposition issues [7]. Multidetector CT is frequently used in addition to radiographs for the imaging evaluation of a symptomatic THA as this method can detect soft tissue, bone and metal hardware complications. The diagnostic performance of CT for PL can be further improved by metal artifact reduction algorithms (MARs) [8–14]. MRI can also be useful in this setting [15, 16] but requires optimized protocols for MAR with longer acquisition times compared with radiographs and CT with MAR (CT-MAR) [17, 18].

Digital tomosynthesis (DTS) is a recent emerging imaging technique derived from radiographic tomography with various clinical applications described in the literature [19–21]. It provides multiple section planes obtained from several projections of various angles. It has been almost 10 years since the introduction of DTS in THA imaging [22]. Previous studies comparing DTS with conventional radiographs and computed tomography for the diagnosis of PL have suggested a better performance of DTS for PL and osteointegration identification [23–27]. However, these studies were performed without the use state-of-the-art MAR techniques on CT, which has been shown to increase CT diagnostic performance [9].

The aim of this study is to compare the diagnostic performance of DTS with that of conventional radiographs and CT-MAR using surgical results and clinical follow-up as the standard of reference and to propose an optimal strategy in imaging workup of patients with a painful THA.

Material and methods

Patient selection

From January 2012 to January 2016 patients with painful THA that underwent hip DTS were consecutively included in a prospective study approved by the local ethics committee. All patients were over 18 years old and signed an informed consent form. Imaging findings were correlated with surgical findings and with clinical and radiological follow-up. Patients that were treated conservatively without clinical or radiological follow-up 1 year after the end of the inclusion period were excluded.

Imaging

All patients underwent radiographic evaluation (anteroposterior views of the pelvis and anteroposterior and urethral profile views of the hip), anteroposterior DTS and CT-MAR images of the pathological hip.

Conventional radiographs and digital tomosynthesis

Radiographs and DTS were performed using a flat panel detector (Definium 8000; GE Healthcare). Radiographs were obtained with a tube voltage of 75 kV and a variable mA (maximum 800 mA) depending on patient body habitus. DTS acquisitions were performed with 85 kV and 125 mA, with a pixel spacing of 0.2 × 0.2 mm. The source-detector distance was set to 100 cm. There was a movement from -20° to +20° of the x-ray tube for DTS, resulting in 60 coronal slices, obtained in 10 s, reconstructed using filtered back projection. Radiation dose assessment was performed as described by Göthlin and Geijer [26] on a set of five patients not included in image analysis.

CT acquisition

CT images were acquired on a 320 detector-row CT scanner (Aquillion one, Canon Medical Systems). Patients were positioned supine with the hip extended. A helical acquisition was performed with a z-axis coverage starting 3 cm proximal to the acetabular roof and ending 1 cm distal to the lower extremity of the femoral component of the prosthesis. The acquisition parameters were 135 kV and 100–400 mAs depending on patient body habitus, gantry rotation time in 1 s, slice thickness 0.5 mm, FOV 32 cm and matrix 512 × 512. Images were reconstructed in the axial, coronal and sagittal planes with 1.5 mm slice thickness with both bone and soft tissue kernels. Images were reconstructed with a metal artifact reduction algorithm based on single-energy raw-data extrapolation (single energy metal artifact reduction—SEMAR, Canon Medical Imaging) commercialized and available for clinical use [9, 28]. Dose-length product was assessed and effective doses were calculated using a κ coefficient of 0.015 [29].

Image analysis

Images were evaluated independently by two radiologists (R.G. and C.B.), with 4 and 6 years of clinical experience, blinded to clinical and surgical patient data. Imaging studies were anonymized and displayed in random order on a dedicated workstation (Vitrea console, Vital Solutions—Canon

Medical Systems) with soft tissue and bone window settings of W400/L50 and W2700/L350 respectively. A training session with radiographs, DTS and CT-MAR was performed among the readers with images from ten patients not included in this study.

Images were evaluated in four readout sessions (conventional radiographs only, DTS only, CT-MAR only and radiographs associated with DTS) with at least a 2-week interval between them. The presence or absence of cement was noted for each imaging technique and for each prosthetic component. Regardless of the image modality, image analysis was based on the evaluation of each zone of Gruen and De Lee and Charnley for the presence or absence of periprosthetic radiolucency (Fig. 1) [30, 31]. Only coronal and sagittal CT images were used to allow a direct inter-modality correlation of the Gruen and De Lee and Charnley zones.

Periprosthetic radiolucent lines (radiolucent bone lysis adjacent to the prosthetic components) wider than 2 mm found within two or more adjacent Gruen or De Lee and Charnley zones were considered diagnostic of PL. For presence or absence of PL, all available images were evaluated (anteroposterior and profile radiographic views, anteroposterior DTS views and all CT-MAR reformats). The number of radiolucent zones (RLZs) for each imaging technique was calculated. For the intermodality comparison of the number of RLZs, only the coronal CT-MAR reformats and anteroposterior radiographic views were used to allow a direct comparison with DTS images (anteroposterior only).

The presence of bone or prosthetic material fractures was also assessed. Imaging findings were correlated with surgical signs of PL. Patients were considered PL negative if they had a negative radiological follow-up of at least 1 year, an alternative diagnosis explaining patient's symptoms or no surgical evidence of PL.

Statistical analysis

The sensitivity, specificity, positive and negative predictive value for each reader and each imaging technique for PL detection in the acetabular and femoral prosthetic components separately or in association were calculated. Sensitivities and specificities of each image modality were compared using the McNemar test. Interobserver agreement was assessed using the Cohen kappa test. Kappa values of 0–0.20 were considered slight agreement, 0.21–0.40 fair, 0.41–0.60 moderate, 0.61–0.80 substantial and 0.81–1 excellent agreement. The significance of age differences in the groups evaluated was assessed with the Mann-Whitney U Test. Paired comparison of the number of RLZs found for each imaging technique was performed by using a paired Student's t test. The threshold of statistical significance was set to $p < 0.05$.

Results

We selected 63 patients; 14 were excluded because they did not undergo surgery and/or were lost during follow-up. Thus, the final population consisted of 49 patients (23 female, 26 male, male/female ratio = 1.1) with a mean age of 65.1 ± 13.5 years ranging from 27–87 years and a BMI of 28.01 ± 6 ranging from 19.8–42.6. Thirty-four patients had an uncemented prosthesis; 15 had a cemented one. There were 21 cases of PL (10 in cemented and 11 in uncemented prostheses), 12 of both acetabular and femoral component loosening and 9 of acetabular component only, in 15 males and 6 females, with significantly more males than females (p = 0.047). On the other hand, there was no significant difference between the age (67 ± 11.4 versus 63.11 ± 14.8 years, p = 0.242) and the BMI (28.44 ± 5.79 versus 27.62 ± 5.91, p = 0.632) of patients with and without PL.

Kappa values for each modality and each prosthetic component are shown in Table 1. Compared with conventional radiographs and DTS, the interobserver agreement was higher with CT-MAR regardless of the prosthetic component considered (0.39 versus 0.52 and 0.83 respectively). When conventional radiographs and DTS were evaluated in association, the interobserver agreement improved (0.64) but remained lower than that of CT-MAR. The prosthetic component had a considerable impact on kappa values. The interobserver agreement of DTS was slightly lower than for the other modalities in the femoral component (0.53 versus 0.69 for both conventional radiographs and CT-MAR). The interobserver agreement was much lower in the acetabular compared with the femoral component with conventional radiographs (0.18 versus 0.69). This difference was less striking with DTS (0.49 versus 0.53) and reversed with CT-MAR (0.87 versus 0.69). When conventional radiographs and DTS were evaluated in association, the interobserver agreement in the acetabular component improved (0.18 versus 0.49 versus 0.6 in conventional radiographs, DTS and both in association respectively) but remained lower than that of CT-MAR (0.87).

Sensitivity, specificity, positive and negative predictive values of each imaging technique for the diagnosis of PL for both readers in the acetabular component, femoral component and both are shown in Table 2. The sensitivity of conventional radiographs and DTS for the detection of PL, alone or in association, was poor, varying from 33.3–57.1%. The sensitivity was slightly better for PL detection in the acetabular component with respect to the femoral component varying from 47.6–57.1% and 33.3–41.6% respectively. For both readers, CT-MAR was more sensitive (90.4–95.2%) than the other imaging modalities for the diagnosis of acetabular PL (for reader 1, p = 0.026 for reader 1 for each imaging technique, for reader 2, p =

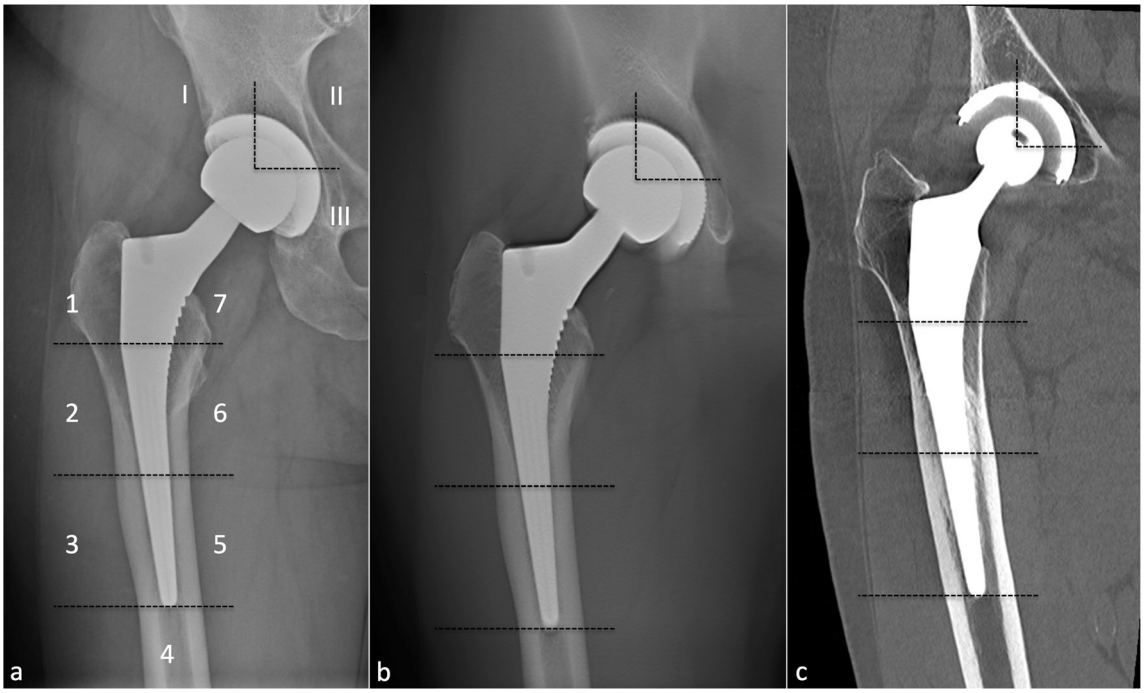

Fig. 1 Normal AP radiograph (**a**), digital tomosynthesis (**b**) and coronal CT-MAR reformat (**c**) of a right sided uncemented THA in a 53-year-old female. Gruen zones 1 to 7 and DeLee and Charnley zones I, II, III are delineated and annotated in (**a**). Gruen zones 8 to 14 were evaluated on lateral radiographs and sagittal CT-MAR reformats (not shown here)

0.005 compared with radiographs, 0.016 compared with DTS and 0.026 compared with radiographs + DTS) (Fig. 2). The diagnostic performance of CT-MAR for the diagnosis of femoral PL was lower (66.6–75%) and there was no statistically significant difference with respect to conventional radiographs and DTS ($p > 0.2$). Specificity values for PL detection were high regardless of the imaging modality and prosthetic component (94.5–100%). In one case the diagnosis of PL was not reached with DTS because of the absence of lateral views. In this case PL could be confirmed with conventional radiographs.

Table 1 Interobserver agreement for each imaging technique according to each component and for global prosthesis loosening

Technique and prosthesis component	Interobserver agreement (kappa)
Radiographs/femoral component (FC)	0.6928
Radiographs/acetabular component (AC)	0.1833
Tomosynthesis/FC	0.5385
Tomosynthesis/AC	0.4974
CT-MAR/FC	0.697
CT-MAR/AC	0.8757
Radiographs + tomosynthesis/FC	0.6928
Radiographs + tomosynthesis/AC	0.6023
Radiographs/both components	0.3929
Tomosynthesis/both components	0.5275
CT-MAR/both components	0.8363
Radiographs + tomosynthesis/both components	0.6442

The number of RLZs depicted for each reader, each imaging technique and each prosthetic component is shown in Table 3. For both readers, more peri-prosthetic RLZs were depicted with CT-MAR than with radiographs (mean 6.18 ± 8.65 versus 2.69 ± 5.53 positive RLZs per patient) ($p = 0.0003$), DTS (mean 4.43 ± 5.49 versus 1.77 ± 3.44 positive RLZs per patient) ($p = 0.0001$) (Fig. 3) and both conventional radiographs and DTS (mean 6.18 ± 8.65 versus 3.02 ± 6.01 positive RLZs per patient) ($p = 0.0011$). A similar number or RLZs were identified with conventional radiographs and DTS (mean RLZs per patient of 1.78 ± 3.44 and 1.88 ± 3.33 respectively) ($p = 0.506$). However, a significantly higher number of RLZs were identified when these two modalities were associated (mean RLZs per patient of 3.02 ± 6.01 versus 2.69 ± 5.53, $p < 0.004$, for radiographs alone, and mean RLZs per patient of 2.29 ± 3.83 vs 1.77 ± 3.44, $p = 0.0008$, for DTS alone).

For radiographs, the mean area-product dose was 1.835 ± 0.575 Gy.cm^2 (range = 1.12–2.74) and the mean effective dose 0.532 ± 0.167 mSv (range = 0.325–0.795). For DTS, the mean area-product dose was 0.742 ± 0.308 Gy.cm^2 (range = 0.33–1.1) and the mean effective dose 0.215 ± 0.089 mSv (range = 0.139–0.319). For CT-MAR, the mean dose-length product was 579.1 ± 177.766 mGy.cm (range = 340.2–1584.53) and the mean effective dose 0.8686 ± 0.266 mSv (range = 0.5103–2.3767).

Table 2 Diagnostic performance of each imaging technique for each reader for acetabular component, femoral component and global prosthesis loosening

	Reader 1	Reader 2	Reader 1	Reader 2	Reader 1	Reader 2	Reader 1	Reader 2
Acetabular component	Se	Se	Sp	Sp	PPV	PPV	NPV	NPV
Radiographs	57.14	33.3	96.43	100	92.31	100	75	66.67
Tomosynthesis	57.14	42.86	96.43	100	92.31	100	75	70
CT-MAR	95.24*	90.48*	96.43	96.43	95.24	95	96.43	93.1
Radiographs + tomosynthesis	57.14	47.62	96.43	100	92.31	100	75	71.74
Femoral component	Se	Se	Sp	Sp	PPV	PPV	NPV	NPV
Radiographs	41.67	33.33	97.3	100	83.33	100	83.72	82.22
Tomosynthesis	25	33.33	100	100	100	100	80.43	82.22
CT-MAR	66.67	75	97.3	94.59	88.89	81.82	90	92.11
Radiographs + tomosynthesis	41.67	33.33	97.3	100	83.3	100	83.72	82.22
Prosthesis Loosening	Se	Se	Sp	Sp	PPV	PPV	NPV	NPV
Radiographs	51.52	33.33	96.92	100	89.47	100	79.75	74.71
Tomosynthesis	45.45	39.39	98.46	100	93.75	100	78.05	76.47
CT-MAR	84.85*	84.85*	96.92	95.38	93.33	90.32	92.65	92.54
Radiographs + Tomosynthesis	51.52	42.42	97.01	100	89.47	100	80.25	77.38

Se Sensitivity, *Sp* Specificity, *PPV* Positive predictive value, *PVN* Predictive negative value

*Statistically significant values

Discussion

Radiographs presented a fair reproducibility and poor sensitivity for PL detection. The use of DTS (alone or in association) did not improve the sensitivity of conventional radiographs for the diagnosis of PL. The best interobserver agreement however, was reached when conventional radiographs were associated with DTS, with kappa values improving from fair to substantial (kappa 0.64). Additionally, a significantly greater number of RLZs were identified when conventional radiographs were combined with DTS compared with radiographs and DTS alone (10–20% increase). CT-

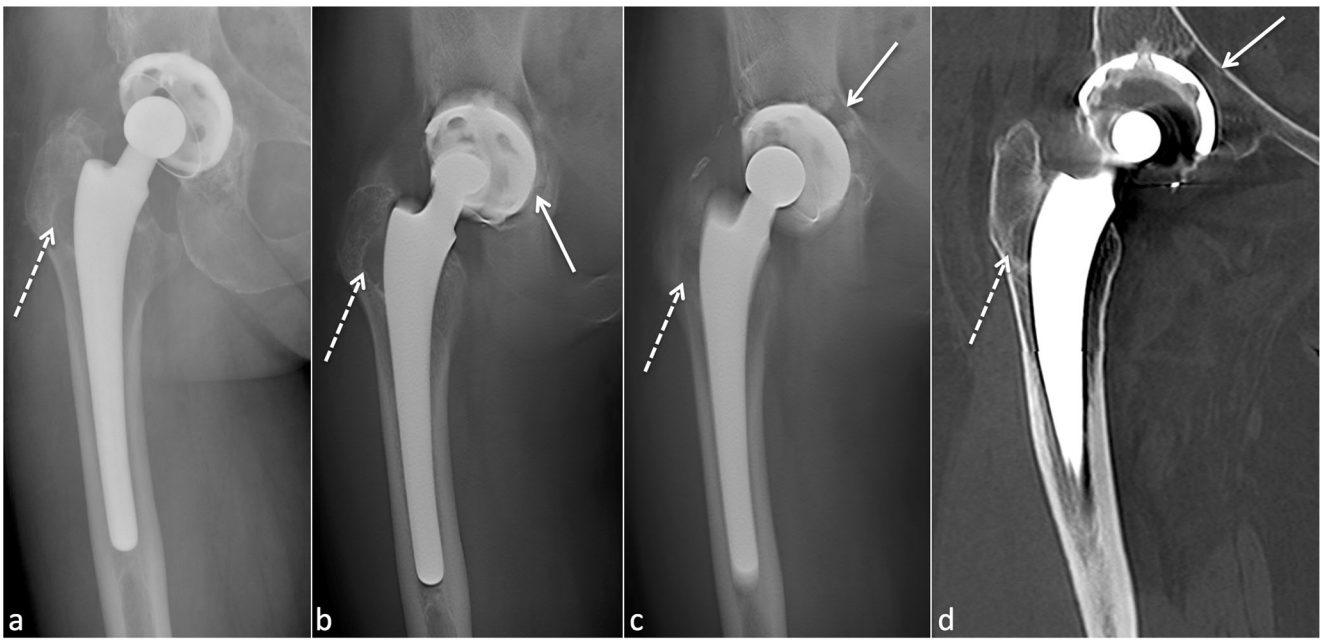

Fig. 2 AP radiograph (**a**), digital tomosynthesis (**b** and **c**) and coronal CT-MAR reformat (**d**) of a right-sided uncemented THA in a 60-year-old male with acetabular cup loosening. Acetabular osteolysis (white arrow) is not seen on radiograph but is well depicted with tomosynthesis as it extends into zone II and III and is also seen on CT-MAR. Osteolysis in zone 1 is also depicted by the three imaging modalities (dotted white arrow)

Table 3 Number of radiolucent zones (RLZs) depicted by each reader for each imaging technique

	Radiographs		DTS		CT-MAR		Radiographs + DTS	
	R1	R2	R1	R2	R1	R2	R1	R2
Frontal view	56	37	44	42	112	99	61	46
Profile view	22	18	NA	NA	50	35	22	18
Total per reader	78	55	44	42	162	134	83	64
Total for R1 + R2	133		86		296		147	

"Frontal views" corresponds to anteroposterior radiographs views, anteroposterior tomosynthesis views and coronal CT-MAR reformats. "Profile views" corresponds to urethral profile radiograph views and sagittal CT-MAR reformats. "NA" means not applicable, as no tomosynthesis profile views were performed in this study. Total per reader and for reader 1 and 2 are shown in the two bottom lines

MAR presented a significantly higher sensitivity than and similar specificity to conventional radiographs and DTS combined with a higher interobserver agreement. The effective dose of CT-MAR was similar to that of the conventional radiograph-DTS combination (0.86 mSv and 0.74 mSv respectively). These results indicate that despite the improvements from the addition of DTS over the performance of conventional radiographs, CT-MAR is the best image modality for the diagnosis of PL. Thus, in clinical practice, DTS can be recommended in association with conventional radiographs for the initial evaluation of a painful THA as these methods can be more available than CT-MAR. Furthermore, DTS can be performed at the same time as the radiograph and does not disrupt patient workflow. Nonetheless, when this initial evaluation proves inconclusive (no signs of PL or no abnormality explaining patient symptoms), the use of CT-MAR is warranted.

The prosthetic component (femoral versus acetabular) had an impact on the performance of all image modalities evaluated for the diagnosis loosening, a drop in sensitivity (more noticeable with DTS and CT-MAR, particularly for reader 1) for the diagnosis of femoral PL compared with acetabular PL. This reduction in sensitivity in the femoral component was identified despite a higher interobserver agreement with conventional radiographs and DTS for PL identification in this region compared with the acetabulum. The lower interobserver agreement for the evaluation of acetabular PL with conventional radiographs and DTS could be explained by the more complex anatomy of the acetabulum with respect to the proximal femur, which could lead to superimposition pitfalls.

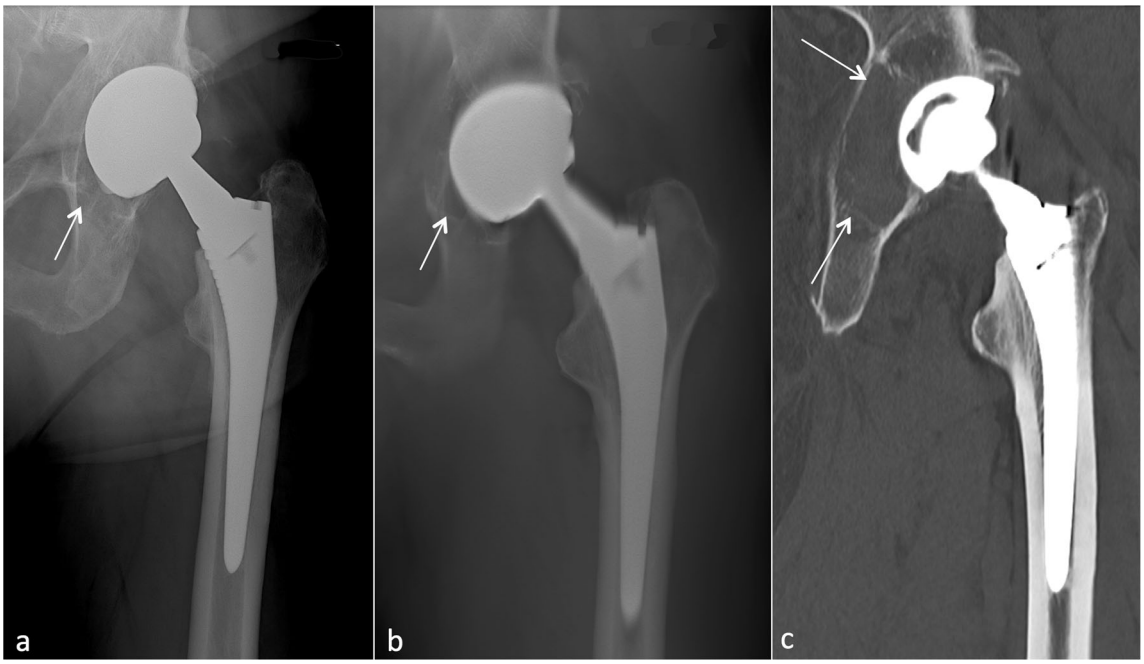

Fig. 3 AP radiograph (**a**), digital tomosynthesis (**b**) and coronal CT-MAR reformat (**c**) of a left-sided uncemented THA in a 55-year-old male with acetabular cup loosening. Note the doubtful osteolysis in zone III on AP radiograph (white arrow), much better seen with tomosynthesis (white arrow). The extent of osteolysis is clearly better depicted with CT-MAR and is finally present in zone I, II and III (white arrows)

Moreover, a similar drop in sensitivity in the femoral component was noted with CT-MAR (66–75% versus 90–95% at the femoral and acetabular components respectively). These findings are in favor of a worse clinic-radiological correlation for the diagnosis of femoral PL in the presence of RLZs.

Although conventional radiographs remain the initial imaging modality for the evaluation of patients with a painful THA, the low performance of this method for the diagnosis of PL is in accordance with previous literature reports [32]. The presented results differ from those of Tang et al who reported better performance of DTS compared with CT for the diagnosis of PL using a DTS MAR algorithm [27]. Additionally, in a 2008 phantom study, Gomi et al suggested DTS was less susceptible to artifacts than CT in the presence of metal [22]. These differences are likely related to the different reconstruction algorithms used for DTS and CT-MAR in the different studies performed. Metal artifact reduction and low dose algorithms can be applied to this technique with good clinical outcomes and less cost and radiation dosage than CT [27, 33–41]. For instance, in the study of Tang et al, DTS with MAR algorithms had a mean effective dose six times lower than that of CT [27]. Moreover, with different reconstructions methods in a prosthesis phantom study, Gomi et al found that radiation levels could be decreased by 20% without compromising image quality [24], as did Becker et al in DTS of the wrist, reducing the radiation dose up to 70% without a significant effect on the visibility of anatomic structures, by modulating acquisition parameters [39]. In addition, Simoni et al declared that DTS of the feet was about half the price of CT and 1/5 of contrast-enhanced MRI in this setting [36]. However, in our opinion, the potential gain in image quality when using MAR algorithms for DTS is insufficient to offset a roughly 40% increase in the sensitivity for acetabular PL seen when DTS was compared with CT-MAR. Finally, the delivered and effective doses presented were lower than in previous reports for radiographs, DTS and CT examinations [25, 27]. These differences can be explained at least partially by the constant improvements in detector performance and in the efficiency of iterative reconstruction algorithms [9, 42–45].

Our study has a few limitations. Most importantly, the study population was relatively small with a limited number of PL cases. Further studies in larger populations are required to confirm the presented findings and to evaluate diagnostic performance in specific prosthesis types such as cemented and uncemented prostheses [26]. Imaging follow-up was not possible as patients were not followed up with all three imaging modalities evaluated. Thus, prosthesis migration and progression in the size of RLZs, which are known diagnostic criteria for loosening, were not evaluated in this study, which could have underestimated the diagnostic performance of the image methods studied [32, 46]. Tang et al found better sensitivities for DTS than for CT for PL diagnosis, but they did not use CT-MAR and TS benefit from metal artifact reduction algorithms (TMAR) [27]. In our study, DTS did not, underscoring the relevance comparing CT-MAR and TMAR in this setting. Some authors suggested that DTS is a potential help for readers with less clinical experience [47, 48]. This issue was not assessed in this study.

In conclusion, DTS can assist in the diagnosis of PL because of its better interobserver agreement than conventional radiographs, especially for acetabular component loosening. CT-MAR, however, remains the technique with the highest diagnostic performance with higher sensitivity and better interobserver agreement. Thus, radiographs should be coupled with DTS for the initial evaluation of patients with a painful THA. CT-MAR can be recommended in cases of inconclusive initial evaluation (radiographs + DTS). An alternative approach, in institutions where CT-MAR is readily available, would be to use this method for the initial evaluation of symptomatic THA, although this strategy could be less cost effective.

Funding The authors state that this work has not received any funding.

Compliance with ethical standards

Guarantor The scientific guarantor of this publication is Prof. Alain Blum.

Conflict of interest The authors of this manuscript declare relationships with the following companies: non-remunerated research contract with Toshiba Medical Systems for the development and clinical testing of post processing tools for MSK CT (Prof. Alain Blum and Prof. Pedro Augusto Teixeira). The other authors have no potential conflicts of interest to disclose.

Statistics and biometry One of the authors has significant statistical expertise (Dr. Romain Gillet).

Informed consent Written informed consent was obtained from all subjects (patients) in this study.

Ethical approval Institutional Review Board approval was obtained.

Methodology
- prospective
- diagnostic study
- performed at one institution

References

1. Nemes S, Gordon M, Rogmark C, Rolfson O (2014) Projections of total hip replacement in Sweden from 2013 to 2030. Acta Orthop 85:238–243
2. Labek G, Thaler M, Janda W, Agreiter M, Stöckl B (2011) Revision rates after total joint replacement: cumulative results from worldwide joint register datasets. J Bone Joint Surg Br 93:293–297
3. Delaunay C, Hamadouche M, Girard J, Duhamel A; SoFCOT Group (2013) What are the causes for failures of primary hip arthroplasties in France? Clin Orthop Relat Res 471:3863–3869

4. Duffy PJ, Masri BA, Garbuz DS, Duncan CP (2005) Evaluation of patients with pain following total hip replacement. J Bone Joint Surg Am 87:2565–2575
5. Patel AR, Sweeney P, Ochenjele G, Wixson R, Stulberg SD, Puri LM (2015) Radiographically silent loosening of the acetabular component in hip arthroplasty. Am J Orthop (Belle Mead NJ) 44: 406–410
6. Eklund K, Jonsson K, Lindblom G et al (2004) Are digital images good enough? A comparative study of conventional film-screen vs digital radiographs on printed images of total hip replacement. Eur Radiol 14:865–869
7. Claus AM, Engh CA Jr, Sychterz CJ, Xenos JS, Orishimo KF, Engh CA Sr (2003) Radiographic definition of pelvic osteolysis following total hip arthroplasty. J Bone Joint Surg Am 85:1519–1526
8. Blum A, Meyer JB, Raymond A et al (2016) CT of hip prosthesis: new techniques and new paradigms. Diagn Interv Imaging 97:725–733
9. Gondim Teixeira PA, Meyer JB, Baumann C et al (2014) Total hip prosthesis CT with single-energy projection-based metallic artifact reduction: impact on the visualization of specific periprosthetic soft tissue structures. Skeletal Radiol 43:1237–1246
10. Roth TD, Maertz NA, Parr JA, Buckwalter KA, Choplin RH (2012) CT of the hip prosthesis: appearance of components, fixation, and complications. Radiographics 32:1089–1107
11. Chen Z, Pandit H, Taylor A, Gill H, Murray D, Ostlere S (2011) Metal-on-metal hip resurfacings—a radiological perspective. Eur Radiol 21:485–491
12. Laukamp KR, Lennartz S, Neuhaus VF et al (2018) CT metal artifacts in patients with total hip replacements: for artifact reduction monoenergetic reconstructions and post-processing algorithms are both efficient but not similar. Eur Radiol. https://doi.org/10.1007/s00330-018-5414-2
13. Lee YH, Park KK, Song HT, Kim S, Suh JS (2012) Metal artefact reduction in gemstone spectral imaging dual-energy CT with and without metal artefact reduction software. Eur Radiol 22:1331–1340
14. West AT, Marshall TJ, Bearcroft PW (2009) CT of the musculoskeletal system: what is left is the days of MRI? Eur Radiol 19:152–164
15. Agten CA, Sutter R, Dora C, Pfirrmann CW (2017) MR imaging of soft tissue alterations after total hip arthroplasty: comparison of classic surgical approaches. Eur Radiol 27:1312–1321
16. Kretzschmar M, Nardo L, Han MM et al (2015) Metal artefact suppression at 3 T MRI: comparison of MAVRIC-SL with conventional fast spin echo sequences in patients with hip joint arthroplasty. Eur Radiol 25:2403–2411
17. Fritz J, Lurie B, Miller TT, Potter HG (2014) MR imaging of hip arthroplasty implants. Radiographics 34:E106–E132
18. Fritz J, Lurie B, Miller TT (2013) Imaging of hip arthroplasty. Semin Musculoskelet Radiol 17:316–327
19. Blum A, Noël A, Regent D, Villani N, Gillet R, Gondim Teixeira P (2018) Tomosynthesis in musculoskeletal pathology. Diagn Interv Imaging 99:423–441
20. Machida H, Yuhara T, Tamura M et al (2016) Whole-body clinical applications of digital tomosynthesis. Radiographics 36:735–750
21. Geijer M, Gunnlaugsson E, Götestrand S, Weber L, Geijer H (2017) Tomosynthesis of the thoracic spine: added value in diagnosing vertebral fractures in the elderly. Eur Radiol 27:491–497
22. Gomi T, Hirano H (2008) Clinical potential of digital linear tomosynthesis imaging of total joint arthroplasty. J Digit Imaging 21:312–322
23. Gomi T, Hirano H, Umeda T (2009) Evaluation of the X-ray digital linear tomosynthesis reconstruction processing method for metal artifact reduction. Comput Med Imaging Graph 33:267–274
24. Gomi T, Sakai R, Goto M, Watanabe Y, Takeda T, Umeda T (2016) Comparison of reconstruction algorithms for decreasing the exposure dose during digital tomosynthesis for arthroplasty: a phantom study. J Digit Imaging 29:488–495
25. Guo S, Tang H, Zhou Y, Huang Y, Shao H, Yang D (2017) Accuracy of digital tomosynthesis with metal artifact reduction for detecting osteointegration in cementless hip arthroplasty. J Arthroplasty. https://doi.org/10.1016/j.arth.2017.12.037
26. Göthlin JH, Geijer M (2013) The utility of digital linear tomosynthesis imaging of total hip joint arthroplasty with suspicion of loosening: a prospective study in 40 patients. Biomed Res Int 2013:1–6
27. Tang H, Yang D, Guo S et al (2016) Digital tomosynthesis with metal artifact reduction for assessing cementless hip arthroplasty: a diagnostic cohort study of 48 patients. Skeletal Radiol 45:1523–1532
28. Chang YB, Xu D, Zamyatin AA (2012) Metal artifact reduction algorithm for single energy and dual energy CT scans. In: 2012 IEEE Nuclear Science Symposium and Medical Imaging Conference Record (NSS/MIC), Anaheim, CA, 2012, pp. 3426–3429
29. Christner JA, Kofler JM, McCollough CH (2010) Estimating effective dose for ct using dose–length product compared with using organ doses: consequences of adopting International Commission on Radiological Protection Publication 103 or dual-energy scanning. AJR Am J Roentgenol 194:881–889
30. DeLee JG, Charnley J (1976) Radiological demarcation of cemented sockets in total hip replacement. Clin Orthop Relat Res 20–32
31. Gruen TA, McNeice G, Amstutz HC (1979) "Modes of failure" of cemented stem-type femoral components: a radiographic analysis of loosening. Clin Orthop Relat Res 141:17–2723
32. Abrahams JM, Kim YS, Callary SA et al (2017) The diagnostic performance of radiographic criteria to detect aseptic acetabular component loosening after revision total hip arthroplasty. Bone Joint J 99-B:458–464
33. Wu T, Moore RH, Rafferty EA, Kopans DB (2004) A comparison of reconstruction algorithms for breast tomosynthesis. Med Phys 31:2636–2647
34. Mermuys K, De Geeter F, Bacher K et al (2010) Digital Tomosynthesis in the detection of urolithiasis: diagnostic performance and dosimetry compared with digital radiography with MDCT as the reference standard. AJR Am J Roentgenol 195: 161–167
35. Ha AS, Lee AY, Hippe DS, Chou SH, Chew FS (2015) Digital tomosynthesis to evaluate fracture healing: prospective comparison with radiography and CT. AJR Am J Roentgenol 205:136–141
36. Simoni P, Gérard L, Kaiser MJ et al (2015) Use of Tomosynthesis for detection of bone erosions of the foot in patients with established rheumatoid arthritis: comparison with radiography and CT. AJR Am J Roentgenol 205:364–370
37. Canella C, Philippe P, Pansini V, Salleron J, Flipo RM, Cotten A (2011) Use of tomosynthesis for erosion evaluation in rheumatoid arthritic hands and wrists. Radiology 258:199–205
38. Ottenin MA, Jacquot A, Grospretre O et al (2012) Evaluation of the diagnostic performance of tomosynthesis in fractures of the wrist. AJR Am J Roentgenol 198:180–186
39. Becker AS, Martini K, Higashigaito K, Guggenberger R, Andreisek G, Frauenfelder T (2017) Dose reduction in tomosynthesis of the wrist. AJR Am J Roentgenol 208:159–164
40. Machida H, Yuhara T, Tamura M et al (2012) Radiation dose of digital tomosynthesis for sinonasal examination: comparison with multi-detector CT. Eur J Radiol 81:1140–1145
41. Lacout A, Thariat J, Hajjam ME, Marcy PY (2013) Insight into osteo-articular digital tomosynthesis: a pictorial essay: osteo-articular digital tomosynthesis. J Med Imaging Radiat Oncol 57: 45–49

42. Lombard C, Gervaise A, Villani N et al (2018) The impact of dose reduction in quantitative kinematic CT of ankle joints using a full model-based iterative reconstruction algorithm: a cadaveric study. AJR Am J Roentgenol 210:396–403
43. Gervaise A, Osemont B, Lecocq S et al (2012) CT image quality improvement using adaptive iterative dose reduction with wide-volume acquisition on 320-detector CT. Eur Radiol 22:295–301
44. Gervaise A, Teixeira P, Villani N, Lecocq S, Louis M, Blum A (2013) CT dose optimisation and reduction in osteoarticular disease. Diagn Interv Imaging 94:371–388
45. Gervaise A, Osemont B, Louis M, Lecocq S, Teixeira P, Blum A (2014) Standard dose versus low-dose abdominal and pelvic CT: comparison between filtered back projection versus adaptive iterative dose reduction 3D. Diagn Interv Imaging 95:47–53
46. Kim YS, Abrahams JM, Callary SA et al (2017) Proximal translation of > 1 mm within the first two years of revision total hip arthroplasty correctly predicts whether or not an acetabular component is loose in 80% of cases: a case-control study with confirmed intra-operative outcomes. Bone Joint J 99-B:465–474
47. Hayashi D, Xu L, Gusenburg J et al (2014) Reliability of semiquantitative assessment of osteophytes and subchondral cysts on tomosynthesis images by radiologists with different levels of expertise. Diagn Interv Radiol 20:353–359
48. Tucker L, Gilbert FJ, Astley SM et al (2017) Does reader performance with digital breast tomosynthesis vary according to experience with two-dimensional mammography? Radiology 283:371–380